Healthcare Analytics 4 (2023) 100265

Contents lists available at ScienceDirect

Healthcare Analytics

journal homepage: www.elsevier.com/locate/health

A real-time deep learning approach for classifying cervical spine fractures

Showmick Guha Paul, Arpa Saha, Md Assaduzzaman *

Dept. of CSE, Daffodil International University, Dhaka, Bangladesh

A R T I C L E   I N F O

Handling editor:Madijd Tavana

Keywords:
Cervical spine fracture
Fracture detection
Transfer learning
Deep learning
Computed tomography

A B S T R A C T

The first seven vertebrae of our spine are called the cervical spine. It supports the weight of our head, encloses and safeguards our spinal cord, and permits a variety of head motions. The seven cervical vertebrae are joined at the rear of the bone by a kind of joint known as a facet joint. These joints enable us to move our necks forward, backward, and twist. Fractures of the cervical spine are a medical emergency that may lead to lifelong paralysis or even death. If left untreated and undetected, these fractures can worsen over time. Using computed tomography, a cervical spine fracture in individuals can be accurately diagnosed. Given the scarcity of research on the practical use of deep learning methods in detecting spine fractures in persons, it is imperative to address this gap. This study uses a dataset containing fracture and normal cervical spine computed tomography images. This study proposed modified transfer-learning-based MobileNetV2, InceptionV3, and Resnet50V2 models. An ablation study was also conducted to determine the optimal custom layers for models and data augmentation techniques. In addition, evaluation metrics have been used to analyze and compare the model's performance. Among all the approaches, MobileNetV2 with augmentation has achieved the highest accuracy of 99.75%. Furthermore, the best-performing model has been deployed in a smartphone-based Android application.

1. Introduction

Diagnostic imaging is crucial for the treatment of spinal diseases [1]. Over the past few decades, there has been a dramatic increase in spine imaging procedures due to the increasing prevalence of spinal disease associated with an aging population and the widespread availability of computed tomography (CT). Fractures of the cervical spine can occur in people of all ages, but they are more prevalent in men. The most common cause of cervical spine fracture is falling, followed by car accidents, motorcycling, and diving, causing 5–10% instant death [2,3]. Furthermore, cervical spine fractures are caused by abnormal movement or a combination of abnormal motions, such as hyperflexion, rotation, hyperextension, lateral bending, and axial loading of the spinal column [4]. A cervical spine injury has the potential to be linked with a high morbidity and death rate [5], and a delay in the identification of an unstable fracture that leads to insufficient immobilization may result in a catastrophic deterioration in the neurologic function that has terrible consequences [6–9]. Examining the cervical spine with imaging is thus an essential initial step in assessing patients with multidetector and trauma. CT has been established as the standard of care imaging tool to examine cervical spine injuries [10]. Patients who have sustained an injury to their cervical spine have a lower risk of morbidity and death if they get prompt diagnosis and treatment. The cervical spine is the source of cervicogenic headache (CGH), a chronic secondary headache that may originate in the neck or occipital area [11]. Sources of CGH include all structures innervated by the C1 through C3 nerve roots [12].

Furthermore, depending on which vertebra is fractured, each individual with a cervical spine fracture will experience slightly different symptoms [13]. By leveraging the capabilities of machine learning (ML) and deep learning (DL), cervical spine-related and other diverse tasks

* Corresponding author.
E-mail addresses: showmick.cse@gmail.com (S. Guha Paul), arpasaha.cse@gmail.com (A. Saha), assaduzzaman.cse@diu.edu.bd (M. Assaduzzaman).

https://doi.org/10.1016/j.health.2023.100265
Received 30 December 2022; Received in revised form 19 September 2023; Accepted 19 September 2023
Available online 24 September 2023

within the medical sector can be efficiently undertaken, heralding substantial advancements and opportunities for improvement. ML and DL algorithms, including vanilla convolutional neural networks, Fourier-CNN, and residual networks, for image segmentation in magnetic resonance imaging scans, can identify anomalies related to cardiovascular diseases [14]. By employing deep neural networks for feature extraction from CT scan images, researchers can achieve an early and accurate diagnosis of lung cancer and improved diagnostic accuracy, including the ability to distinguish between malignant tumors and benign [15]. DL in the medical health sector offers innovative solutions. For instance, the use of EEGnet architecture for stress detection enables early identification and prevention of health problems [16]. The research explores the application of modified DL models using the pre-trained VGG-19 models with an improved augmentation technique for classifying lung cancer biopsy images [17]. There is also potential for the ultrasonic imaging-based DL model to be an effective method of monitoring the healing of bone after fracture surgery [18]. DL-based models can also be utilized for the automatic detection and positioning system of fresh rib fractures, which can outperform radiologists in terms of sensitivity [19]. Using plain radiographs and employing DL methods, fractures, bone mineral density and fracture risk can be identified and evaluated [20]. Moreover, DL facilitates sentiment analysis of user-generated multimedia data, such as tweets related to diseases like monkeypox, enhancing our understanding of public reactions and promoting disease awareness and surveillance [21]. Various other problems, such as anxiety problems, can be classified at early stages using ML algorithms [22]. Introducing automatic X-ray image segmentation techniques, compression fractures can be detected and evaluated in X-ray images [23]. Using a deep CNN model, osteopenia and osteoporosis can be classified by lumbar spine X-ray images, demonstrating the potential for screening these conditions non-invasively [24]. DL also extends to real-time health monitoring for athletes using wearable technology and recurrent neural networks, resulting in enhanced conditioning and performance while reducing the risk of injuries [25]. This application encompasses continuous remote monitoring, analysis of medical data from wearable devices, and patient feedback, enabling real-time health condition prediction, ultimately improving patient outcomes while reducing healthcare costs [26]. Furthermore, lightweight CNN algorithms can be used to detect pneumonia with a deployable diagnostic-aid solution, which can aid in developing remote healthcare systems [27].

A severe kind of medical malpractice often involved with doctors is misdiagnosis. Because of a misdiagnosis or a delayed diagnosis can worsen a patient's health. A wrong diagnosis could also cause spending more time and energy treating problem. A misdiagnosis may even result in death in some circumstances. Furthermore, many diagnostic tests may be needed to diagnose certain diseases accurately. DL models can tackle the issue by assisting doctors in the early detection of cervical spine fractures.

Furthermore, manual evaluation of patient data requires much time and is fraught with the risks of diagnostic analysis mistakes and inaccurate information. On the other hand, health applications can eliminate all these potentially deadly obstacles the patient could face. Furthermore, the patient's current state of health can be digitally managed via an application. This makes it easier for medical professionals to conduct proper treatment of patients with conditions of the cervical spine. Therefore, this study follows some objectives to address the current issue of cervical spine fracture detection.

- To develop and validate a robust cervical spine fracture detection model using a state-of-the-art DL-based model, utilizing a dataset comprising fracture and normal cervical spine CT images.
- To conduct an ablation study to identify the optimal custom layers and data augmentation techniques that enhance the performance of the DL models in detecting cervical spine fractures.
- To build a real-time application that can aid in early detection to prevent worsening complications.

The development of DL models has recently been in progress, and rapid and accurate prediction has recently been widely accessible. As a result, experts are now able to save time using DL models to detect issues related to medical conditions. Thus, in the study, transfer learning-based DL models have been proposed to detect cervical spine fractures, and an application based on Android has been developed to aid doctors in detecting cervical spine fractures.

The following are some of the primary muscles that connect to our cervical spine[28–32] (see Appendix A).

Fig. A.1. Muscles of the cervical spine.

1.1. *Ligaments of our cervical spine*

The bones of our cervical spine are connected by ligaments, which contribute to the stability of our cervical spine. The primary ligaments of the cervical spine are as follows.

1.1.1. *Anterior longitudinal ligament*

The anterior longitudinal ligament is a strong fibrous band that runs along the front surface of the cervical vertebrae, extending from the base of our skull down to the bottom of the spine. This ligament plays a crucial role in stabilizing the vertebral column and preventing excessive backward movement of the neck. By providing essential support and limiting hyperextension, the anterior longitudinal ligament helps maintain the natural curvature of the cervical spine and prevents potential injuries that could result from excessive backward bending or hypermobility [33].

1.1.2. *Posterior longitudinal ligament*

The posterior longitudinal ligament is a tough and flexible band that originates at the second cervical vertebra and runs down the entire length of the back surface of the cervical vertebrae until it reaches the base of the skull. This ligament is crucial in preventing excessive forward movement of the neck and provides essential support to the vertebral column [33]. As a stabilizing structure, the posterior longitudinal ligament resists hyperflexion of the cervical spine, helping to maintain the natural curvature of the neck and preventing potential injuries that could result from excessive forward bending or hypermobility.

1.1.3. *Ligamentum flava*

These ligaments line the posterior surface of the inside opening of each vertebra, which is where our spinal cord travels through our body. These ligaments wrap around and shield our spinal cord to protect it from the back.

Fig. 1 illustrates the human spine structure and the name of the spine according to region. Disks are one of the most essential elements in the structure of the cervical spine. The "shock absorber cushions" between each vertebra are called cervical disks. There is a total of six disks located between the seven vertebrae that make up the cervical region. During physical activity, the disks protect our neck from the forces exerted on it and make it easier for us to flex and swivel our head.

The nerves of the cervical spine are one of the important elements which are reasonable for communication and proper body functioning.

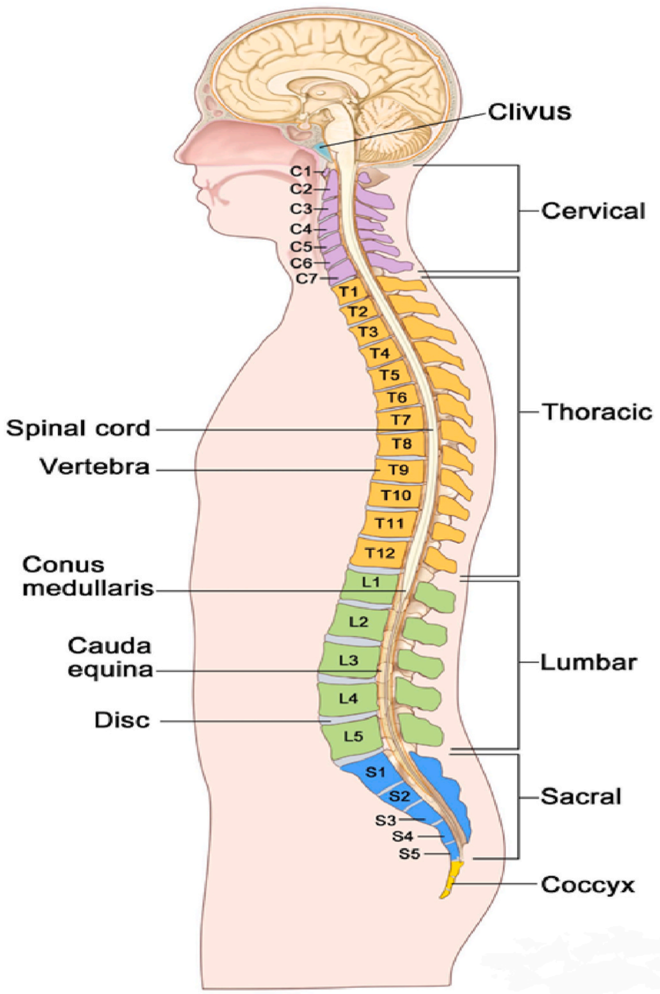

Fig. 1. Cervical spine in human body [34].

From Fig. 2, in the cervical region of our spine, there are eight pairs of spinal nerves that leave the body via tiny holes (foramen) between every pair of vertebrae. Their designations range from C1 to C8 [35,36].

1.2. Cervical nerves C1, C2 and C3

It regulates the rotation of the head and neck in all directions. The C2 nerve transmits sensory information from the brain to the top of our heads. The feeling from C3 might be felt on the side of our face and the top of our head.

1.3. Cervical nerve 4

As one of the nerves responsible for diaphragmatic function, it regulates the movement of our upper shoulders. A portion of our neck, shoulders, and upper arms receive sensation from C4.

1.4. Cervical nerve 5

It has control over the deltoids in our shoulders as well as the biceps in our arms. The C5 nerve gives us feeling from the top of our upper arm all the way down to our elbow.

1.5. Cervical nerve 6

It regulates the flexor muscles of the forearm and contributes to the control of the biceps. C6 is responsible for providing feeling to the side of our thumb, both in our forearm and in our hand.

1.6. Cervical nerve 7

It has control over our triceps as well as the muscles that extend the wrist. The C7 nerve gives us sensation all the way down the back of our arms into our middle fingers.

1.7. Cervical nerve 8

Our forearm and pinky side of our hands get sensations from it, and it also controls our hands.

The classification of the cervical spine fracture in an image is a challenging issue to solve, recurring specialist medical knowledge. In addition, information that is readily accessible to the public spine data is quite restricted, which makes it much more challenging to make advancements toward automated cervical spine fracture classification. The following is the key contribution that our research has contributed.

I. The studies implement a state-of-the-art cervical fracture C.T. image dataset, obtained from the RSNA cervical spine fracture detection challenge.
II. Various TL-based deep learning models consisting of custom layers have been applied in the study.
III. An ablation study has been conducted to improve the performance of the models, and numerous techniques of data augmentation have been identified.
IV. To aid medical professionals, the most effective model's has been implemented into the Android application.

The following are the remaining portions of this research: related research on the topic of classifying cervical spine fractures is included in section 2. The modified transfer learning-based models' architecture is discussed in section 3 for classifying the cervical spine fracture, as well as dataset and prepressing of dataset. Section 4 showcases the study's experimental evaluation results and analysis, along with the outcomes derived from the implemented models. Furthermore, the deployment procedure of Android-based application and discussion is described. The study's conclusion and the future perspective are highlighted in section 5.

2. Related work

Cervical spine fractures are one of the most significant concerns in healthcare due to their potential to be linked with a high morbidity and death rate, their impact on neurologic function, and the patient's well-being. In this context, ML and DL models have emerged as promising methods to assist healthcare professionals in detecting those fractures accurately. This section will analyze prior, varied studies on this subject, critically analyzing and synthesizing existing research work to provide context and insights.

The human spine, comprising the cervical, thoracic, and lumbar regions, is crucial in supporting the body's structure and protecting the spinal cord. The cervical spine, consisting of seven vertebrae, is particularly susceptible to fractures and injuries. In recent years, a surge in research has leveraged the power of DL in medical imaging and diagnostics for the cervical spine and the overall human spine. Small et al. [37] led this charge by pioneering the use of convolutional neural networks (CNNs) for detecting cervical spine fractures in C.T. scans, demonstrating DL versatility. Simultaneously, Chłąd and Ogiela [38] explored cloud-based computation to enhance cervical spine fracture detection, highlighting the synergy between DL and cloud resources. Boonrod et al. [39] conducted a comprehensive investigation into using DL for C-spine injury evaluation from lateral neck radiographs. Concurrently, Naguib et al. [40] classified cervical spine fractures and dislocations, employing refined, pre-trained deep models and saliency

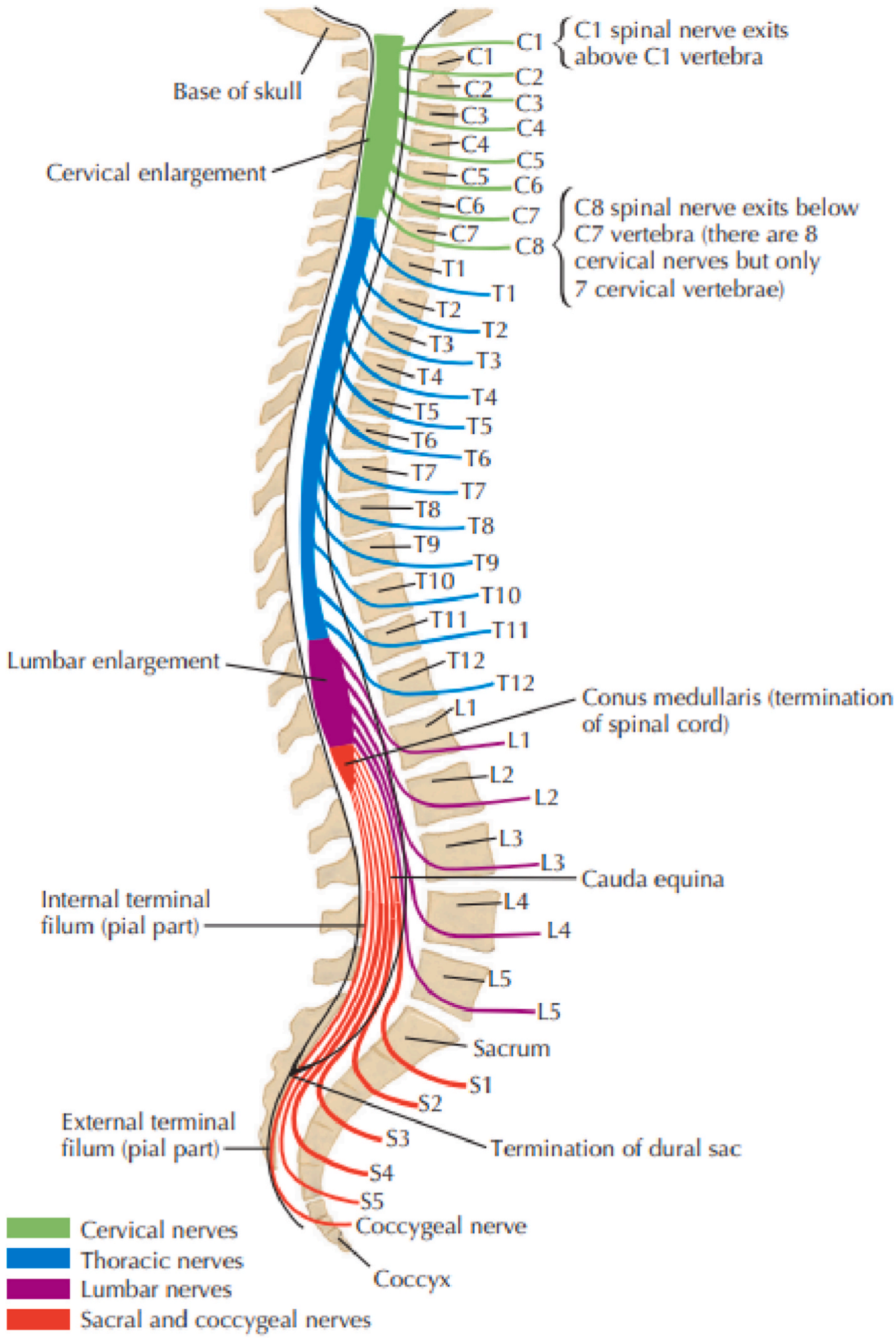

Fig. 2. Anatomical overview of cervical nerves and their structural organization [35].

maps for improved fracture detection. Salehinejad et al. [41] advanced the field with deep sequential learning for cervical spine fracture detection in C.T. imaging, while Jakubicek et al. [42] enriched spine imaging with a deep-learning-based automatic spine centerline detection method tailored for C.T. data. Weng et al. [43] employed DL to recognize whole-spine sagittal alignment, while Karanam et al. [44] supervised musculoskeletal imaging through DL algorithms for fracture detection and classification. Furthermore, Kassem et al. [45] introduced an explainable transfer learning-based deep model for pelvis fracture detection, enhancing interpretability.

In addressing the challenge of cervical spine fracture detection, medical research has witnessed the customization and training of ML and DL models tailored to specific datasets. These models encompass a spectrum of cutting-edge architectures, including CNN, vision transformers (ViT), YOLO network models, and deep neural networks like AlexNet, GoogleNet, and ResNet [37–40]. These sophisticated frameworks are meticulously crafted to scrutinize and interpret a diverse range of medical imaging modalities, such as C.T. scans, X-rays, and radiographs, with the primary objective of precise and automated fracture identification [38,39,41].

Custom models are specifically designed to tackle unique and

Table 1
The cervical spine fracture dataset.

Class id	Class name	Count	Training	Testing
0	fracture	2100	1900	200
1	normal	2100	1900	200

complex challenges, such as the detection of cervical spine fractures, bone cancer identification, and vertebral compression fractures. These models offer several advantages, including optimized performance, enhanced accuracy, and interpretability, all tailored to the specific medical context. However, a noticeable gap exists in some studies that rely solely on traditional or pre-trained models, potentially missing out on the benefits that custom models can provide. Yi et al. [46] applied DL techniques but did not utilize custom models, while others, like the study by Boonrod et al. [39], employed traditional methods without incorporating custom models. The absence of custom models in these studies represents an opportunity to investigate the role of custom models in achieving even higher accuracy and efficiency in diagnosing medical conditions [39,46].

To perform cervical and other types of spine-related work, a wide range of dataset sizes is utilized, reflecting the variability in data availability and utilization in the field of medical image analysis using DL. For instance, Small et al. [37] employed a dataset consisting of 665 images for their cervical spine fracture detection study. This dataset size, while relatively small, yielded an accuracy of 92.00%. In contrast, Chład and Ogiela [38] leveraged the extensive RSNA 2022 cervical spine fracture detection challenge dataset, which likely encompassed a much larger number of cases. With this dataset, they achieved an impressive accuracy of 98.00% using ViT models. However, the study did not provide a direct comparison of ViT models with traditional CNN methods. Boonrod et al. [39] encountered the challenge of a small dataset of 229 radiographs by employing objected detection-based YOLO network models for cervical spine injury detection, achieving accuracy and sensitivity rates of 75.00% and 80.00%, respectively. In contrast, Naguib et al. [40] demonstrated exceptional accuracy and sensitivity rates of 99.56% and 99.33%, respectively, for cervical spine injuries. The authors trained the model on a dataset containing 2009 X-ray images (530 CS dislocation, 772 CS fractures, and 707 normal images). Salehinejad et al. [41] incorporated natural language processing elements into their deep CNN model for cervical spine fracture detection but achieved a comparatively lower accuracy of 79.18% on the balanced (104 positive and 104 negative cases) and imbalanced (104 positive and 419 negative cases) test datasets, respectively. Jakubicek et al. [42] achieved a remarkable accuracy of 90.00% for spinal centerline detection, but their study relied on a relatively small dataset of 130 CT images, which could potentially affect the generalization of the models. Maras et al. [47] worked with a dataset comprising 161 normal lateral cervical radiographs and 170 lateral cervical radiographs with osteoarthritis and cervical degenerative disc disease. Their pre-trained VGG-16 network achieved accuracy, sensitivity, specificity, and precision rates of 93.9%, 95.8%, 92.0%, and 92.0%, respectively. A recurring challenge in the realm of cervical spine fracture detection, evident across these studies [37,47–50], is the limited size of the available datasets. While larger datasets like the RSNA 2022 dataset have enabled impressive achievements [38], many investigations have been hampered by their relatively small sample sizes [37,39,41]. This constraint poses a significant hurdle to the field as it can impact the robustness and generalization of developed ML and DL models.

Despite being an important issue in human medical science, very few studies have been conducted to detect cervical spine-based fractures. Furthermore, among the studies, only a limited number have achieved higher accuracy, and to the best of our knowledge, none has analyzed the impact of data augmentation techniques and DL models with custom layers for cervical spine fractures and developed a real-time application that can aid health professionals. In addressing this critical gap, our study embarked on an ambitious endeavour, employing a substantial dataset comprising 4200 cervical spine C.T. images, comprising both fracture and normal cases. Leveraging DL techniques by proposing and implementing modified transfer-learning-based models. Our research also delved into an ablation study, meticulously examining and fine-tuning the custom layers of these models while implementing advanced data augmentation techniques to enhance their robustness. Subsequently, we meticulously evaluated and compared the performance of these models, utilizing a spectrum of rigorous evaluation metrics. To enhance the practical utility of our findings, we have successfully deployed the most proficient model within a smartphone-based Android application. This innovative approach bridges a critical research gap in the timely and accessible detection of cervical spine fractures and also holds the promise of mitigating the severe consequences associated with cervical spine features medical emergencies.

Table 2
Hyperparameter for image data augmentation.

Techniques	Parameter
Shear range	0.2 or 20.00%
Zoom range	0.2 or 20.00%
Horizontal flip	True
Fill mode	Nearest
Width shift range	0.1 or 10%
Height shift range	0.1 or 10%
Rotation range	15 or 15°

3. Proposed methodology and system architecture

3.1. Dataset

The research has been conducted using the "spine fracture prediction from C.T″ dataset, which consists of cervical spine fracture C.T. images [51]. The dataset is divided into two sections: a "train" folder and a "Val" (validation) folder, which consists of two classes: normal cervical spine images and fractured cervical spine images. The dataset consists of 4200 images, whereas the train folder has 1900 fracture images and 1900 normal images (see Table 1). From the training image, 10.00% of the image is randomly chosen for validation purposes using the ImageDataGenerator library. The test dataset contains 400 images, 200 for each class.

3.2. Preprocessing

Prepossessing the data enhances the performance and reduces the time for computation. During the data preprocessing stage, dataset images were resized to a resolution of 224 × 224 pixels. The decision to adopt image dimensions of 224 × 224 in the dataset was based on the fact that a significant proportion of the images in the dataset already possessed these dimensions. Additionally, it is worth noting that utilized deep learning classification models frequently employ this particular

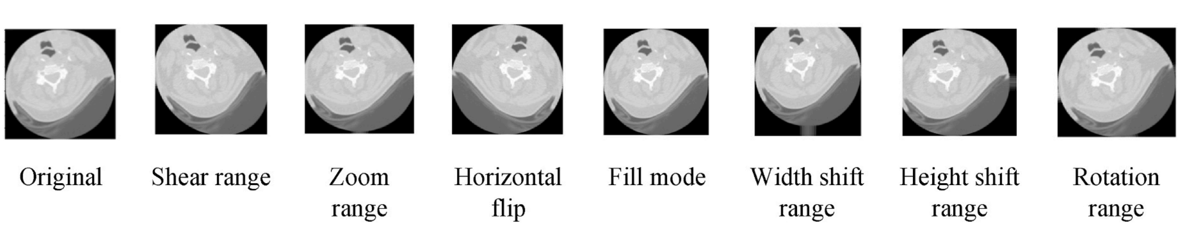

Fig. 3. Cervical sample image after applying augmentation techniques.

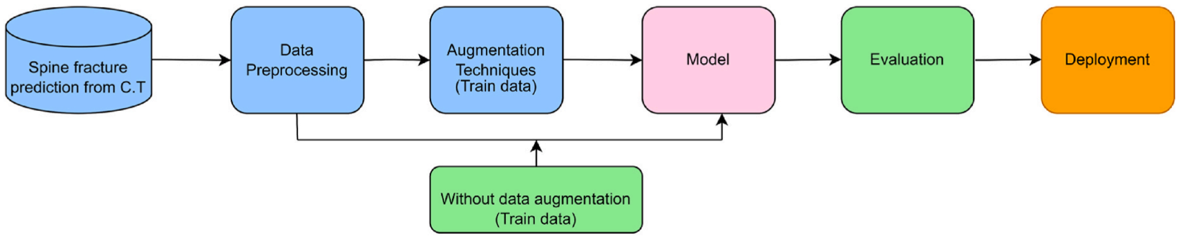

Fig. 4. Diagram of the implementation step.

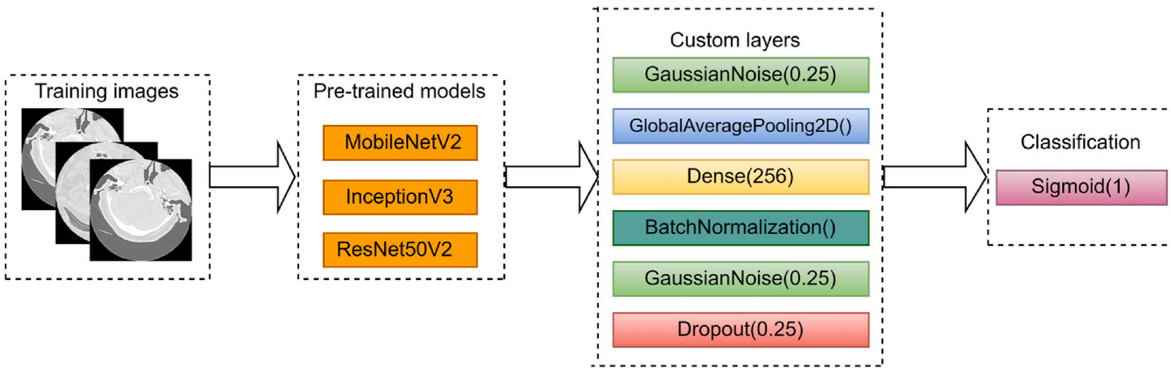

Fig. 5. Applied models architecture.

Table 3
Environmental setup.

Name of the process	S. N.	Performed action
Input	1.	Obtained a dataset consisting of binary class C.T. scans depicting cervical fractures.
Environment Configuration	2.	Anaconda, Jupyter Notebook.
	3.	Import all libraries and necessary packages.
	4.	Images load.
Configuration of directories	5.	Load directories for testing, training, and generate validation (10.00% of training data).
Training and testing	6.	Build transfer learning model using ImsageNet dataset weight.
	7.	Fine tune the models by adding various layers and sigmoid activation function into output layer.
Model compilation	8.	Compile the model using the Adam optimizer and a learning rate of 0.001.
	9.	Set epochs 100 for model fitting.
	10.	Use validation loss monitor as model checkpoint.
	11.	Save the model.
Performance evaluation	12.	Generate confusion matrix and classification report.
	13.	Generate model loss and accuracy reports.
	14.	Generate ROC-AUC curve.
Prediction	15.	Load best model.
	16.	Load random images.
	17.	Predict disease classes.

size as the default input. This image rescaling helps models facilitate faster training time and requires less computational time. The validation dataset has been obtained from the training dataset (10.00%). Various data processing techniques, such as data augmentation and segmentation, can be utilized for effective cervical fracture detection. Although segmentation can aid in isolating individual regions within an image, enabling accurate fracture recognition and localization, segmentation can be computationally intensive and time-consuming, and over-segmentation may cause the image to be noisy, have intensity variations, and not properly distinguish the fracture from real images [52].

Moreover, to enhance the speed and effectiveness of the user experience in real-time applications, it may be beneficial to omit segmentation operations and instead rely on data augmentation techniques to enhance accuracy. As data augmentation can increase the model's ability to generalize, add variability to the data, and minimize data overfitting [53]. Thus, various data augmentation techniques have been applied, selected by performing ablation studies. Fig. 3 illustrates the effect of augmentation techniques on a random dataset sample image. The data augmentation techniques make the models robust and more capable by complexing and enriching the dataset. Additionally, augmentation techniques introduced various transformations in the images and generated fictional data points from pre-existing data. Table 2 presents the augmentation techniques applied in the study.

3.3. Methodology

This study has been conducted in various steps. The dataset, which includes C.T. scan images, has been collected. The preprocessing of the dataset has been done in the follow-up step, which includes resizing the images and applying augmentation techniques in Fig. 4. The studies used a variety of data augmentation techniques that were chosen based on the results of the ablation study. Image quantity and diversity have been increased by performing the data augmentation techniques. Data augmentation techniques help to make models robust and also increase performance. In the following steps, various transfer learning-based algorithms such as MobileNetV2, InceptionV3, and ResNet50V2 have been applied, as among the DL models MobileNetV2, ResNet50V2, and InceptionV3 achieved promising results in detecting various issues and those are some of the most utilized DL models [54,55]. The transfer-learning-based DL models have been implemented using the pre-trained ImageNet weight. The transfer learning-based models have been implemented in two phases. In the transfer learning-based models, the unaugmented dataset was applied first, followed by the augmented dataset in the second phase. The applied models' performance concerning the dataset is evaluated in the following phase. To evaluate the performance, various evaluation metrics such as accuracy, sensitivity, precision, and F1-score have been analyzed and presented. In addition, confusion matrices, accuracy, and validation graphs have been plotted to interpret the behavior of the model. In the final steps, the finest model's has been implemented in the Android-based system, which can assist the medical professional in properly classifying the cervical

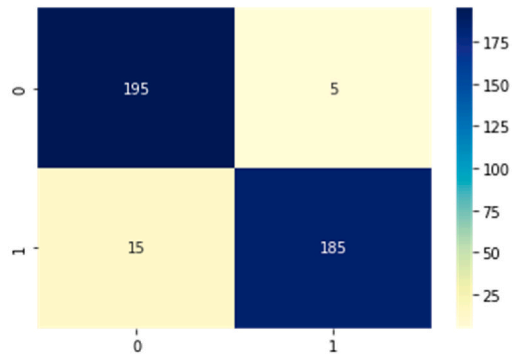

(a) Confusion matrix of the MobileNetV2.

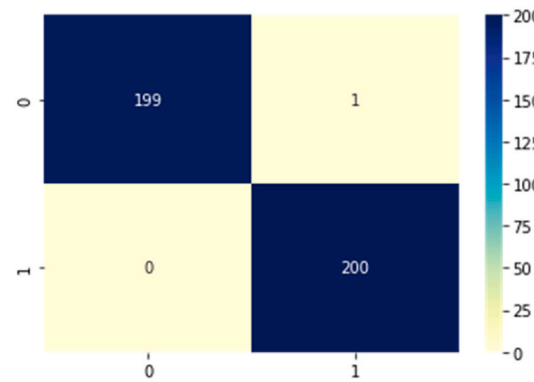

(b) Confusion matrix of the MobileNetV2 with augmentation.

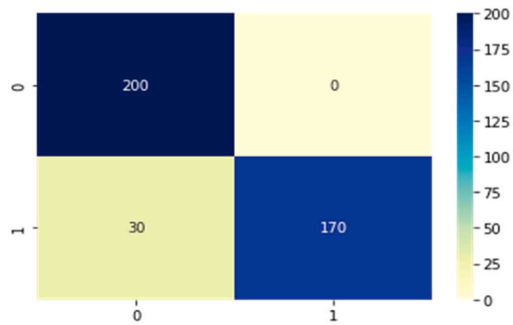

(c) Confusion matrix of the InceptionV3.

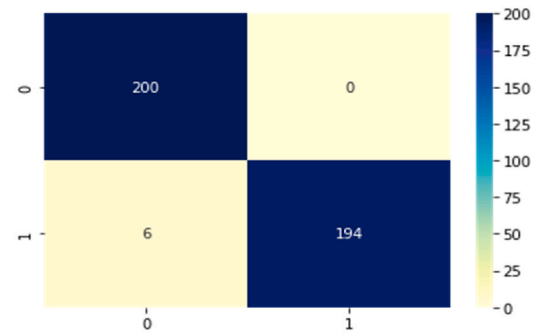

(d) Confusion matrix of the InceptionV3 with augmentation.

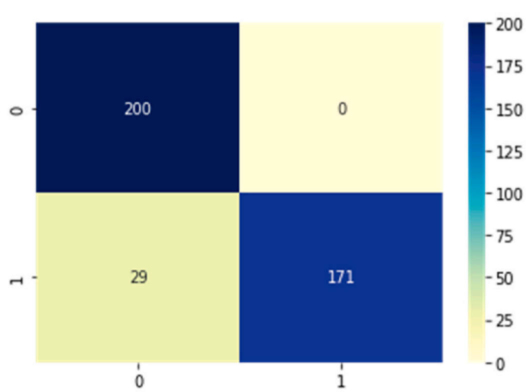

(e) Confusion matrix of the ResNet50V2.

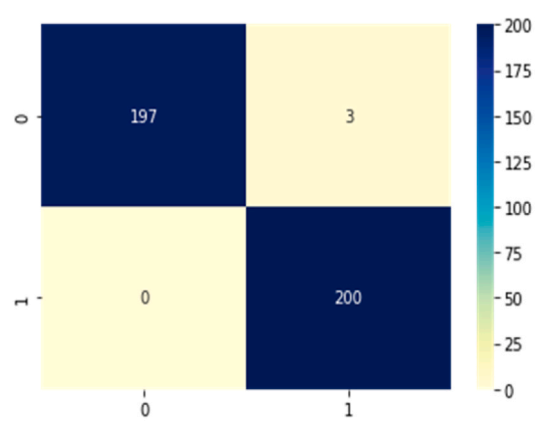

(f) Confusion matrix of the ResNet50V2 with augmentation.

Fig. 6. Confusion matrix for MobileNetV2, InceptionV3, and the ResNet50V2 model (without and with augmentation).

feature scan sample images.

3.4. MobileNetV2

MobileNetV2 is an updated form of MobileNet. It relies on a backward residual structure, where the bottleneck layers connect the residual layers. Lightweight depth-wise convolutions are used in the intermediate expansion layer to filter features and introduce non-linearity. MobileNetV2's overall structure consists of a 32-filter fully convolutional initial layer, followed by 19 residual bottleneck layers. After using the MobileNetV2 pre-train model layer, some custom layers are added to increase performance. The Mobilenetv2 model consists of a total parameter 2,587,201 and a trainable parameter 328,705. Fig. 5 illustrates the custom layers that have been incorporated with the architectural designs of all the models. The sigmoid activation function with one neuron has been used in the output layer for binary classification.

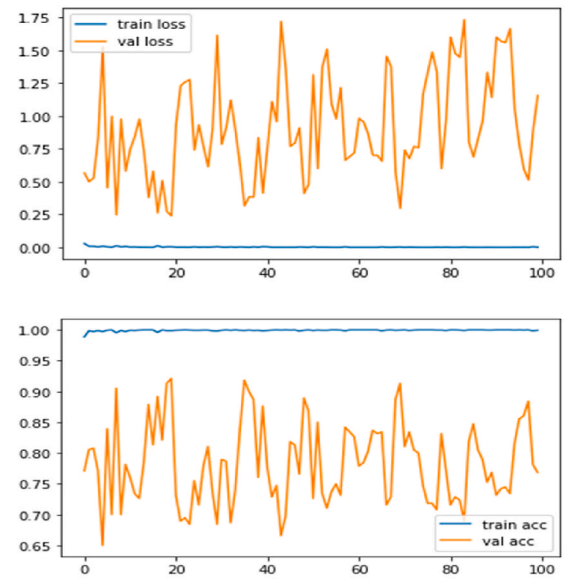

(a) MobileNetV2 accuracy and loss graph.

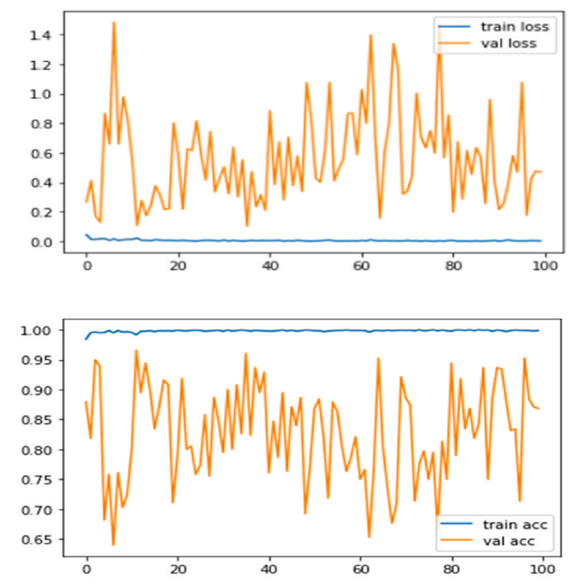

(b) MobileNetV2 with augmentation accuracy and loss graph.

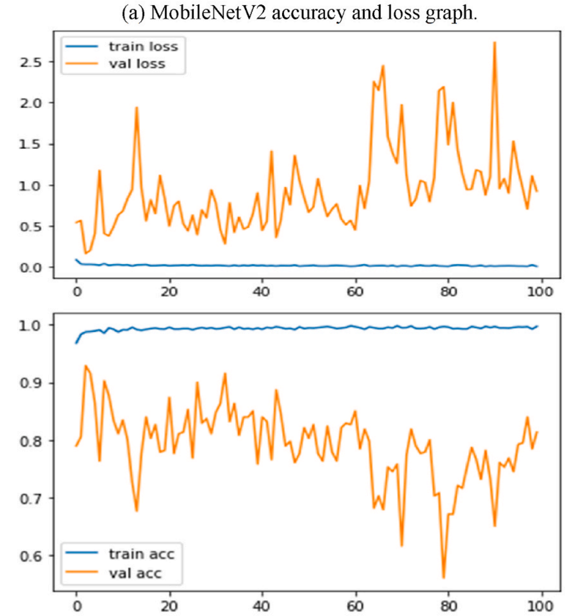

(c) InceptionV3 accuracy and loss graph.

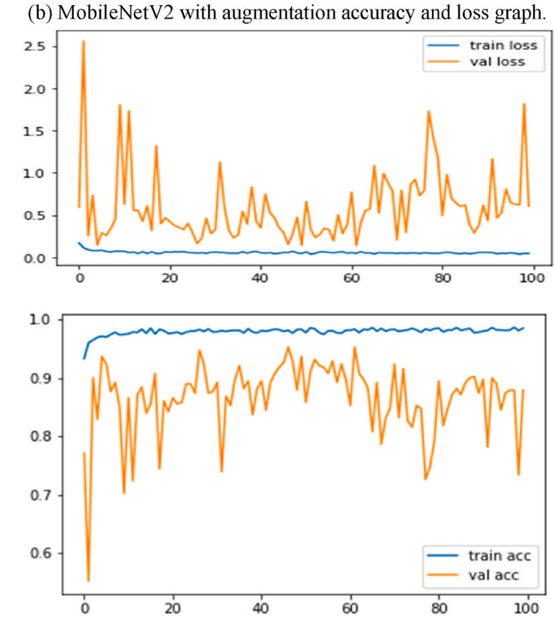

(d) InceptionV3 with augmentation accuracy and loss graph.

Fig. 7. Accuracy and loss graph for MobileNetV2, InceptionV3 and ResNet50V2 model (without augmentation and with augmentation).

3.5. *InceptionV3*

The InceptionV3 architecture is a convolutional neural network and an updated form of the Inception model. Various changes have been made to the InceptionV3 architecture. In InceptionV3, label smoothing has been used. InceptionV3 was developed to accommodate more complex networks without requiring an overwhelming amount of training parameters. InceptionV3 model utilized factorized 7×7 convolutions and an auxiliary classifier to propagate label information and batch normalization. In addition to the existing InceptionV3 architecture, various other custom layers have been added. The InceptionV3 model consists of a total parameter of 22,328,609 and trainable parameter 525,313.

3.6. *ResNet50V2*

ResNet50V2 is an updated version of ResNet50 based on the ResNet architecture and consists of five stages. The ResNet CNN model uses a residual module to overcome the vanishing gradient problem. In ResNet50V2, separate convolution and identity blocks are present, each having three convolution layers. In addition to the ResNet50V2 architecture, some custom layer has been added to the architecture to increase the performance. RestNet50V2 model consists of a total parameter of 24,090,625 and trainable parameters of 525,313.

4. Analysis of experimental evaluation

4.1. *Specification of environment*

The environmental specification is an important aspect of the study

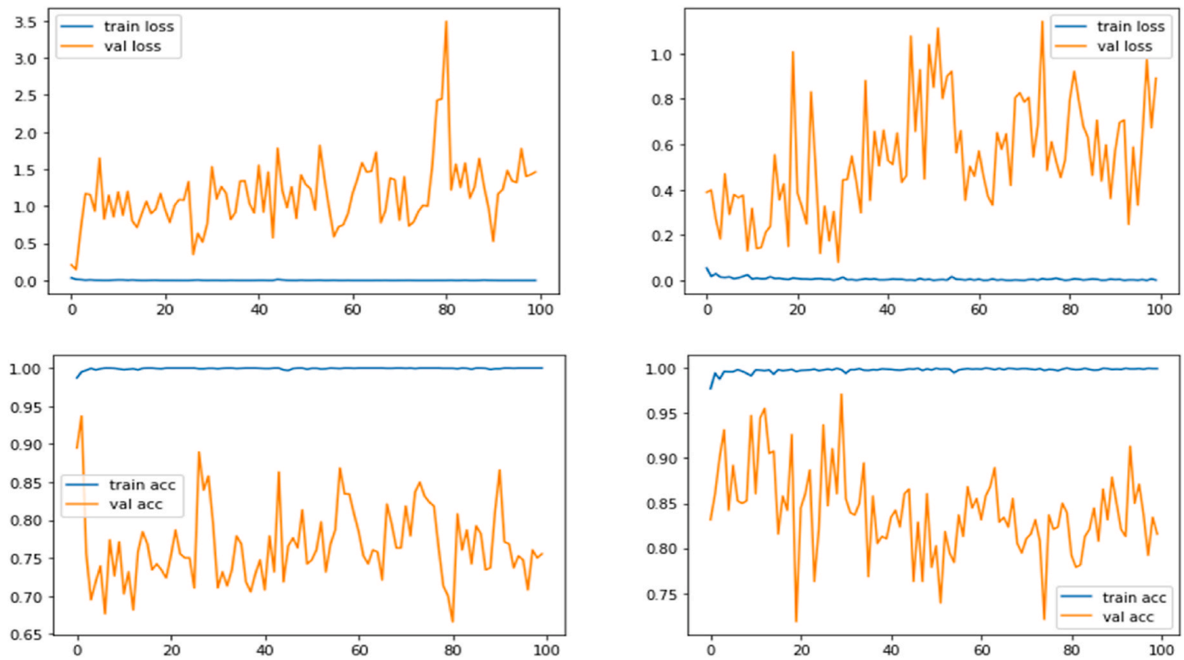

(e) ResNet50V2 accuracy and loss graph.

(f) ResNet50V2 with augmentation accuracy and loss graph.

Fig. 7. (*continued*).

Table 4
Models performance based on evaluation metrics.

Models		Recall	Precision	F1-score
MobileNetV2	Without augmentation	0.9500	0.9511	0.9499
	With augmentation	0.9975	0.9975	0.9975
InceptionV3	Without augmentation	0.9250	0.9347	0.9245
	With augmentation	0.9850	0.9854	0.9849
ResNet50V2	Without augmentation	0.9275	0.9366	0.9271
	With augmentation	0.9925	0.9926	0.9925

Table 5
Models accuracy and loss.

Model		Accuracy		Loss	
	Accuracy	Training	Validation	Training	Validation
MobileNetV2	0.950	0.9988	0.9211	0.0043	0.2402
MobileNetV2 with augmentation	0.9975	0.9991	0.9605	0.0028	0.1024
InceptionV3	0.925	0.9874	0.9289	0.0330	0.1637
InceptionV3 with augmentation	0.985	0.9833	0.9526	0.0473	0.1389
ResNet50V2	0.9275	0.9950	0.9368	0.0132	0.1457
ResNet50V2 with augmentation	0.9925	0.9982	0.9711	0.0064	0.0815

since it describes the experiment's methodology and setup [56]. Table 3 presents the experimental setup used to perform the research work. This study was conducted using the 1.80 GHz processing power of the Core i7-10510U CPU. The system consists of 24 G B. of RAM as well as an NVIDIA graphics card. The system contains a GeForce MX250 NVIDIA graphic card with 4 G B. of dedicated RAM. The applied models were built using Python libraries like Keras and TensorFlow.

4.2. Evaluation metrics

Evaluation metrics are used to determine if a statistical, ML, or DL model is successful. It is essential to apply several assessment criteria to evaluate the best model that research has to offer. Evaluation metrics are essential to guarantee the performance of models. The effectiveness of a model's prediction or classification may be evaluated based on its accuracy, precision, F1-score, and recall value [57].

4.3. Analysis of result and deployment

4.3.1. Analysis of result

The applied model's performance has been analyzed and described in this subsection. The models' confusion matrix, training, validation accuracy, and loss graph have been illustrated. The evaluation metrics' value and the final models' accuracy and loss of training and validation have been computed to compare the models' performances. Finally, other related studies have compared with final models' performance.

The confusion matrix is a popular measure representing predicted and actual values counts. It is applied to measure the performance of binary and multiclass classification. For the classification models, a confusion matrix composed of N × N-shaped matrices is used, which indicates the model's performance or accurately predicted value compared to the actual value.

From Fig. 6, it can be observed that by applying data augmentation techniques to the state-of-the-art models, the performance of the model has increased significantly. Among the models without applying the data augmentation techniques, MobileNetV2 has performed best. By applying the augmentation techniques, the MobileNetV2 model's performance has been significantly increased and has been able to predict approximately all the test samples accurately.

The accuracy and loss graph, also known as the learning curve, is an important element in assessing the performance of DL models. In the learning curve, epochs are plotted in the X-axis and values are plotted in the Y-axis. Dual learning curves were constructed for the DL model during the training process by employing them in both the training and validation dataset. The accuracy graph indicates the training and validation accuracy in terms of the epoch. On the other hand, the loss graph

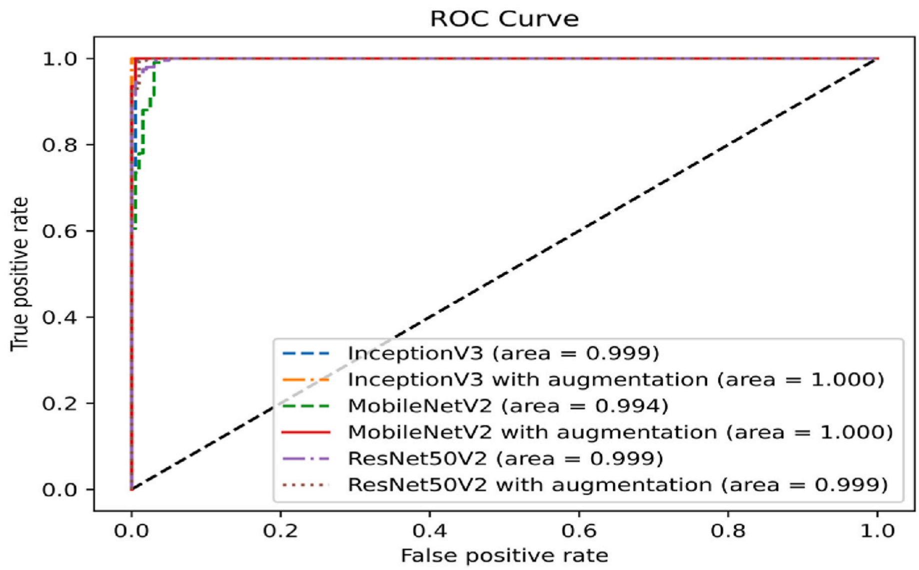

Fig. 8. ROC-AUC curve of applied model.

Table 6
Comparisons of result with related studies.

Reference	Year	Sample size	Used models	Best model (accuracy)	Limitation
Small et al. [37]	2021	665	CNN	CNN (92.00%)	Lower accuracy, no deployment
Boonrod et al. [39]	2022	229	YOLO V2, YOLO V3, YOLO V4	YOLO V4(75.00%)	Lower accuracy, no deployment
Salehinejad et al. [41]	2021	3666	ResNet50 with BLSTM	ResNet50 with BLSTM (79.18%)	Lower accuracy, no deployment
Kim et al. [49]	2021	339	U-Net, R2, SegNet, E-Net, Proposed	Proposed (93.7%)	Lower sample size, no deployment
Our research work	–	4200	MobileNetV2, InceptionV3, ResNet50V2	MobileNetV2 with Augmentation (99.75%)	No web-based deployment

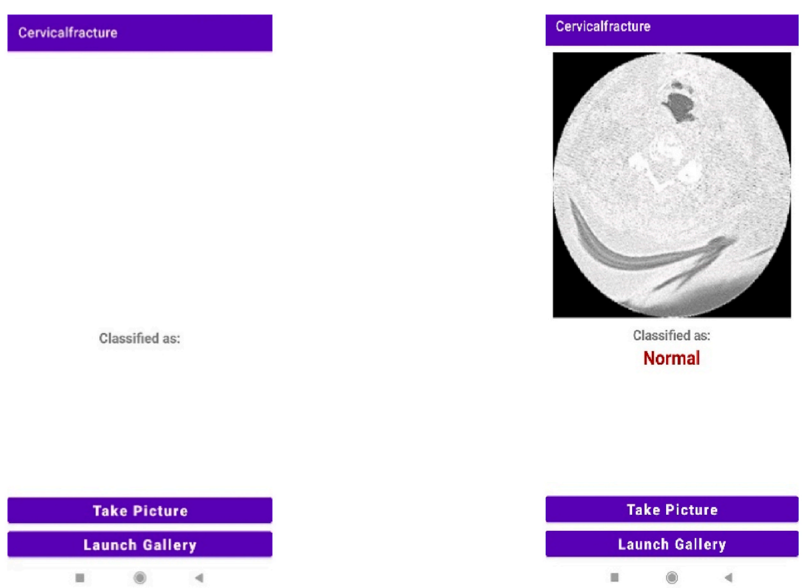

(a) User interface of Android app. (b) Classification result report in Android app.

Fig. 9. Cervical spine fracture disease classification applications.

indicates the model losses it faces during the training process in terms of the epoch.

From Fig. 7, it can be observed that augmentation-based models have achieved better accuracy and face fewer losses compared to models trained without applying augmentation techniques. From Fig. 7(b), it can be observed that MobileNetV2 with augmentation has achieved the most optimal accuracy compared to other model's accuracy graph. Furthermore, MobileNetV2 with augmentation has faced less loss compared to other models.

Accuracy, sensitivity, precision, and F1-score evaluation metrics are employed to evaluate the performance of the applied model. Table 4 describes the performance of the applied model measured via evaluation metrics. InceptionV3 without augmentation achieved the lowest recall value, and ResNet50V2 obtained the higher value. However, after applying augmentation, ResNet50V2 surpasses the InceptionV3. From the table, it can be observed that by applying the augmentation techniques to our state-of-the-art models, the performance of the models has been significantly increased. The importance of evaluation metrics score after applying the augmentation techniques highlights the robustness and effectiveness of selected augmentation techniques. Among the models, MobileNetV2 with augmentation has achieved the highest recall, precision, and F1-score value of 0.9975.

Table 5 describes the models obtained final test accuracy, training and validation accuracy, and loss. Among the models, it can be observed that by employing data augmentation techniques accuracy of the models has been significantly increased. Furthermore, the training and validation accuracy of the model increased by applying augmentation techniques. In addition, the training and validation loss gap has been reduced significantly. Among the models, MobileNetV2 with augmentation has obtained the highest accuracy and faces minimum loss.

Fig. 8 illustrates the applied model's ROC-AUC curve, and it can be observed that the model with augmentation has achieved the most optimal graph with a better AUC score. Among all the models, MobileNetV2 with augmentation has achieved the highest AUC score with the most optimal ROC curve.

Due to diverse challenges and difficulties, a limited number of studies have been conducted to detect cervical spine features. Table 6 describes the related study and compares their result with our research work. The table shows that previously conducted study has obtained lower accuracy, and no instances of real-life implementation have been observed. Our research achieved the highest accuracy and deployed the best model in the Android app to assist medical professionals.

4.3.2. Deployment

Deployment is the process of deploying or implementing the model in an environment that the user can access and use for its intended purpose. Cervical fracture is a critical injury that requires a domain expert to detect. Late detection of fractures can cause blood loss and risk a person's life. Due to a lack of expertise among doctors or medical professionals and a lack of domain specialists, it is critical to develop a system that can assist medical professionals in detecting injuries early and taking the necessary precautions. Therefore, in this cervical spine feature research, one of the major goals is to build an E2E system that can assist doctors and other medical professionals in detecting the cervical spine feature. From Fig. 9, a smartphone application based on Android has been developed to detect cervical spine fractures. To build the Android application, the best-performing model has been saved into the "h5" format and later converted to the TensorFlow lite version file type "tflite" using TFLiteConverter. The application user interface has been created using extensible markup language. The lite TensorFlow model and the backend of the application have been developed using the Java programming language. To load the images into the application, two input method, direct capture and choice from gallery option, has been given. The constructed Android app is compatible with Android versions 12.0 to 5.0. The developed application can be accessed and downloaded from our GitHub repository [58]. As the deployed model has achieved promising accuracy, it can effectively detect cervical spine features.

4.3.3. Discussion

A cervical spine fracture is a serious medical condition involving a break in one or more of the vertebrae located in the neck region. This type of injury can result from severe trauma, leading to significant pain, restricted neck movement, and potential neurological deficits. Therefore, detecting cervical spine fractures early and efficiently is crucial to avoid critical damage or negative effects on our bodies. Over the years, DL methods have played a leading role in the detection of critical medical conditions. Therefore, our study employed the DL methods for detecting cervical spine fractures in individuals. Our study has employed three distinct DL models: MobileNetV2, InceptionV3, and ResNet50V2, with robust custom layers and data augmentation techniques that have been selected by performing an ablation study. The study's implementation results have yielded significant insights and advancements. MobileNetV2 with augmentation emerged as the top-performing model, achieving an impressive accuracy of 99.75%. This achievement represents a substantial advancement in the field, showcasing the effectiveness of the DL model's custom layer and highlighting the importance of data augmentation techniques. Comparing this study's results with related studies, our study demonstrates a remarkable improvement in accuracy and potential deployment. Our models have surpassed the prior studies, which often faced limitations such as lower sample sizes, reduced accuracy, and a lack of deployment strategies. However, it is essential to acknowledge the limitations of our study. The absence of web-based deployment remains a constraint that warrants future exploration. The significance of our study lies in its potential to revolutionize clinical practice by providing a highly accurate and efficient tool for cervical spine fracture diagnosis. Furthermore, this study's methods can aid researchers in detecting various other medical conditions. As cervical spine fractures are a medical emergency, this study's outcomes can offer a vital lifeline, enabling faster, more accurate diagnoses that can ultimately save lives and enhance the quality of patient care.

5. Conclusion

The study uses the DL-based transfer learning model to detect cervical spine fractures. The transfer learning-based MobileNetV2, InceptionV3, and ResNet50V2 models have been utilized to classify cervical spine fractures. An ablation study has been conducted to identify optimal data augmentation techniques and models' custom layers. The results of the applied models have been compared to identify the best-performing model. Among the models, MobileNetV2 has achieved the highest accuracy of 99.75%. Furthermore, the best-performing model has been deployed in an Android-based application to assist doctors and medical professionals. Thus, utilizing state-of-the-art DL technology and practical implementation in Andriod-based applications, this study can contribute to the early and accurate identification of cervical spine fractures and ease the management of critical medical injury.

In the future, findings of the cervical fracture classification research work can serve as a base point for the researcher who wants to conduct research on related fields. Furthermore, real-time web-based applications can be developed that can be used by all types of devices, regardless of the operating system. This study particle implementation can be applied to classify other spine-related fractures. Furthermore, various other techniques and methods, such as segmentation-based classification, feature extraction-based ML model classification, etc., can be implemented to analyze the performance of those techniques.

Declaration of competing interest

The authors declare that they have no known competing financial interests or personal relationships that could have appeared to influence the work reported in this paper.

Data availability

Data will be made available on request.

Acknowledgements (If any)

N/A.

References

[1] J. Splawinski, R. Fox, H. Hall, C.G. Fisher, M. Dvorak, Imaging for spinal surgery, Can. J. Surg. 49 (5) (Oct. 2006) 311–312, discussion 313.

[2] N.M. Beckmann, N.R. Chinapuvvula, X. Zhang, O.C. West, Epidemiology and imaging classification of pediatric cervical spine injuries: 12-year experience at a level 1 trauma center, AJR Am. J. Roentgenol. 214 (6) (Jun. 2020) 1359–1368, https://doi.org/10.2214/AJR.19.22095.

[3] N. Fiedler, U.J.A. Spiegl, J.-S. Jarvers, C. Josten, C.E. Heyde, G. Osterhoff, Epidemiology and management of atlas fractures, Eur. Spine J. 29 (10) (Oct. 2020) 2477–2483, https://doi.org/10.1007/s00586-020-06317-7.

[4] J.V. Modi, S.M. Soman, S. Dalal, Traumatic cervical spondyloptosis of the subaxial cervical spine: a case series with a literature review and a new classification, Asian Spine J 10 (6) (2016) 1058, https://doi.org/10.4184/asj.2016.10.6.1058.

[5] K. Inaba, et al., Cervical spinal clearance: a prospective western trauma association multi-institutional trial, J. Trauma Acute Care Surg. 81 (6) (Dec. 2016) 1122–1130, https://doi.org/10.1097/TA.0000000000001194.

[6] P.M. Poonnoose, G. Ravichandran, M.R. McClelland, Missed and mismanaged injuries of the spinal cord, J. Trauma Inj. Infect. Crit. Care 53 (2) (Aug. 2002) 314–320, https://doi.org/10.1097/00005373-200208000-00021.

[7] R. Izzo, T. Popolizio, R.F. Balzano, A.M. Pennelli, A. Simeone, M. Muto, Imaging of cervical spine traumas, Eur. J. Radiol. 117 (Aug. 2019) 75–88, https://doi.org/10.1016/j.ejrad.2019.05.007.

[8] S. Khanpara, D. Ruiz-Pardo, S.C. Spence, O.C. West, R. Riascos, Incidence of cervical spine fractures on CT: a study in a large level I trauma center, Emerg. Radiol. 27 (1) (Feb. 2020) 1–8, https://doi.org/10.1007/s10140-019-01717-9.

[9] F. Alessandrino, C.M. Bono, C.A. Potter, M.B. Harris, A.D. Sodickson, B. Khurana, Spectrum of diagnostic errors in cervical spine trauma imaging and their clinical significance, Emerg. Radiol. 26 (4) (Aug. 2019) 409–416, https://doi.org/10.1007/s10140-019-01685-0.

[10] M.P. Bernstein, M.G. Young, A.B. Baxter, Imaging of spine trauma, Radiol. Clin. 57 (4) (Jul. 2019) 767–785, https://doi.org/10.1016/j.rcl.2019.02.007.

[11] M. Fernandez, et al., Spinal manipulation for the management of cervicogenic headache: a systematic review and meta-analysis, Eur. J. Pain 24 (9) (Oct. 2020) 1687–1702, https://doi.org/10.1002/ejp.1632.

[12] D.M. Biondi, Cervicogenic headache: mechanisms, evaluation, and treatment strategies, J. Am. Osteopath. Assoc. 100 (9 Suppl) (Sep. 2000) S7–S14.

[13] Neck (Cervical Spine) Fracture." https://www.aftertrauma.org/diagnosis-and-treatment/neck-cervical-spine-fracture (accessed December. 28, 2022).

[14] A. Bhan, P. Mangipudi, A. Goyal, An assessment of machine learning algorithms in diagnosing cardiovascular disease from right ventricle segmentation of cardiac magnetic resonance images, Healthc. Anal. 3 (Nov. 2023), 100162, https://doi.org/10.1016/j.health.2023.100162.

[15] S. Wankhade, S. V, A novel hybrid deep learning method for early detection of lung cancer using neural networks, Healthc. Anal. 3 (Nov. 2023), 100195, https://doi.org/10.1016/j.health.2023.100195.

[16] S. Bhatnagar, S. Khandelwal, S. Jain, H. Vyawahare, A deep learning approach for assessing stress levels in patients using electroencephalogram signals, Decision Anal. J. 7 (Jun. 2023), 100211, https://doi.org/10.1016/j.dajour.2023.100211.

[17] S. Wadekar, D.K. Singh, A modified convolutional neural network framework for categorizing lung cell histopathological image based on residual network, Healthc. Anal. 4 (Dec. 2023), 100224, https://doi.org/10.1016/j.health.2023.100224.

[18] Y. Teng, D. Pan, W. Zhao, Application of deep learning ultrasound imaging in monitoring bone healing after fracture surgery, J. Radiat. Res. Appl. Sci. 16 (1) (Mar. 2023), 100493, https://doi.org/10.1016/j.jrras.2022.100493.

[19] N. Li, et al., An automatic fresh rib fracture detection and positioning system using deep learning, BJR 96 (1146) (Jun. 2023), 20221006, https://doi.org/10.1259/bjr.20221006.

[20] C.-I. Hsieh, et al., Automated bone mineral density prediction and fracture risk assessment using plain radiographs via deep learning, Nat. Commun. 12 (1) (Sep. 2021) 5472, https://doi.org/10.1038/s41467-021-25779-x.

[21] G. Meena, K.K. Mohbey, S. Kumar, K. Lokesh, A hybrid deep learning approach for detecting sentiment polarities and knowledge graph representation on monkeypox tweets, Decision Anal. J. 7 (Jun. 2023), 100243, https://doi.org/10.1016/j.dajour.2023.100243.

[22] E.S. Mohamed, T.A. Naqishbandi, S.A.C. Bukhari, I. Rauf, V. Sawrikar, A. Hussain, A hybrid mental health prediction model using Support Vector Machine, Multilayer Perceptron, and Random Forest algorithms, Healthcare Analytics 3 (Nov. 2023), 100185, https://doi.org/10.1016/j.health.2023.100185.

[23] K.C. Kim, H.C. Cho, T.J. Jang, J.M. Choi, J.K. Seo, Automatic Detection and Segmentation of Lumbar Vertebra from X-Ray Images for Compression Fracture Evaluation, 2019, https://doi.org/10.48550/ARXIV.1904.07624.

[24] B. Zhang, et al., Deep learning of lumbar spine X-ray for osteopenia and osteoporosis screening: a multicenter retrospective cohort study, Bone 140 (Nov. 2020), 115561, https://doi.org/10.1016/j.bone.2020.115561.

[25] W.Y. Alghamdi, A novel deep learning method for predicting athletes' health using wearable sensors and recurrent neural networks, Decision Anal. J. 7 (Jun. 2023), 100213, https://doi.org/10.1016/j.dajour.2023.100213.

[26] K.A. Shastry, A. Shastry, An integrated deep learning and natural language processing approach for continuous remote monitoring in digital health, Decision Anal. J. 8 (Sep. 2023), 100301, https://doi.org/10.1016/j.dajour.2023.100301.

[27] H. Bhatt, M. Shah, A Convolutional Neural Network ensemble model for Pneumonia Detection using chest X-ray images, Healthc. Anal. 3 (Nov. 2023), 100176, https://doi.org/10.1016/j.health.2023.100176.

[28] Cervical Spine (Neck): What It Is, Anat. Disord.," Cleveland Clinic. https://my.clevelandclinic.org/health/articles/22278-cervical-spine (accessed December. 26, 2022)..

[29] L. Cortese, et al., in: Vivo Characterization of the Optical and Hemodynamic Properties of the Human Sternocleidomastoid Muscle through Ultrasound-Guided Hybrid Near-Infrared Spectroscopies, Physiology, preprint, Jun. 2023, https://doi.org/10.1101/2023.06.30.544760.

[30] N. Sollmann, et al., Headache frequency and neck pain are associated with trapezius muscle T2 in tension-type headache among young adults, J. Headache Pain 24 (1) (Jul. 2023) 84, https://doi.org/10.1186/s10194-023-01626-w.

[31] S. Singh, N.K. Choudhary, D. Lalin, V.K. Verma, Bilateral ultrasound-guided erector spinae plane block for postoperative analgesia in lumbar spine surgery: a randomized control trial, J. Neurosurg. Anesthesiol. 32 (4) (Oct. 2020) 330–334, https://doi.org/10.1097/ANA.0000000000000603.

[32] D. Scaturro, et al., Neck pain in fibromyalgia: treatment with exercise and mesotherapy, Biomedicines 11 (3) (Mar. 2023) 892, https://doi.org/10.3390/biomedicines11030892.

[33] M. Lin, et al., A review of finite element modeling for anterior cervical discectomy and fusion, Asian Spine J, Jul. (2023), https://doi.org/10.31616/asj.2022.0295.

[34] Definition of spine - NCI dictionary of cancer terms - NCI. https://www.cancer.gov/publications/dictionaries/cancer-terms/def/spine, Feb. 02, 2011. (Accessed 26 December 2022).

[35] D.L. Felten, M.K. O'Banion, M.S. Maida, Peripheral nervous system, in: Netter's Atlas of Neuroscience, Elsevier, 2016, pp. 153–231, https://doi.org/10.1016/B978-0-323-26511-9.00009-6.

[36] P. Slosar and M. D. Peer-Reviewed, "Cervical Spinal Nerves | Spine-Health.".

[37] J.E. Small, P. Osler, A.B. Paul, M. Kunst, CT cervical spine fracture detection using a convolutional neural network, AJNR Am J Neuroradiol 42 (7) (Jul. 2021) 1341–1347, https://doi.org/10.3174/ajnr.A7094.

[38] P. Chłąd, M.R. Ogiela, Deep learning and cloud-based computation for cervical spine fracture detection system, Electronics 12 (9) (Apr. 2023) 2056, https://doi.org/10.3390/electronics12092056.

[39] A. Boonrod, A. Boonrod, A. Meethawolgul, P. Twinprai, Diagnostic accuracy of deep learning for evaluation of C-spine injury from lateral neck radiographs, Heliyon 8 (8) (Aug. 2022), e10372, https://doi.org/10.1016/j.heliyon.2022.e10372.

[40] S.M. Naguib, H.M. Hamza, K.M. Hosny, M.K. Saleh, M.A. Kassem, Classification of cervical spine fracture and dislocation using refined pre-trained deep model and saliency map, Diagnostics 13 (7) (Mar. 2023) 1273, https://doi.org/10.3390/diagnostics13071273.

[41] H. Salehinejad, et al., Deep sequential learning for cervical spine fracture detection on computed tomography imaging, in: 2021 IEEE 18th International Symposium on Biomedical Imaging (ISBI), IEEE, Nice, France, Apr. 2021, pp. 1911–1914, https://doi.org/10.1109/ISBI48211.2021.9434126.

[42] R. Jakubicek, J. Chmelik, P. Ourednicek, J. Jan, Deep-learning-based fully automatic spine centerline detection in CT data, in: 2019 41st Annual International Conference of the IEEE Engineering in Medicine and Biology Society, EMBC), Berlin, Germany, Jul. 2019, pp. 2407–2410, https://doi.org/10.1109/EMBC.2019.8856528.

[43] C.-H. Weng, Y.-J. Huang, C.-J. Fu, Y.-C. Yeh, C.-Y. Yeh, T.-T. Tsai, Automatic recognition of whole-spine sagittal alignment and curvature analysis through a deep learning technique, Eur. Spine J. 31 (8) (Aug. 2022) 2092–2103, https://doi.org/10.1007/s00586-022-07189-9.

[44] S.R. Karanam, Y. Srinivas, S. Chakravarty, A Supervised Approach to Musculoskeletal Imaging Fracture Detection and Classification Using Deep Learning Algorithms, 2023, https://doi.org/10.24423/CAMES.682.

[45] M.A. Kassem, S.M. Naguib, H.M. Hamza, M.M. Fouda, M.K. Saleh, K.M. Hosny, Explainable transfer learning-based deep learning model for pelvis fracture detection, Int. J. Intell. Syst. 2023 (Jun. 2023) 1–10, https://doi.org/10.1155/2023/3281998.

[46] P.H. Yi, et al., Automated detection and classification of shoulder arthroplasty models using deep learning, Skeletal Radiol. 49 (10) (Oct. 2020) 1623–1632, https://doi.org/10.1007/s00256-020-03463-3.

[47] Y. Maraş, G. Tokdemir, K. Üreten, E. Atalar, S. Duran, H. Maraş, Diagnosis of osteoarthritic changes, loss of cervical lordosis, and disc space narrowing on cervical radiographs with deep learning methods, Jt Dis Relat Surg 33 (1) (Apr. 2022) 93–101, https://doi.org/10.52312/jdrs.2022.445.

[48] S. Gawade, A. Bhansali, K. Patil, D. Shaikh, Application of the convolutional neural networks and supervised deep-learning methods for osteosarcoma bone cancer detection, Healthc. Anal. 3 (Nov. 2023), 100153, https://doi.org/10.1016/j.health.2023.100153.

[49] D.H. Kim, J.G. Jeong, Y.J. Kim, K.G. Kim, J.Y. Jeon, Automated vertebral segmentation and measurement of vertebral compression ratio based on deep learning in X-ray images, J. Digit. Imag. 34 (4) (Aug. 2021) 853–861, https://doi.org/10.1007/s10278-021-00471-0.

[50] H.-D. Chae, et al., Improved diagnostic performance of plain radiography for cervical ossification of the posterior longitudinal ligament using deep learning, PLoS One 17 (4) (Apr. 2022), e0267643, https://doi.org/10.1371/journal.pone.0267643.

[51] V.A. Sairam, Spine Fracture Prediction from C.T, Version 1, 2022, October. https://www.kaggle.com/datasets/vuppalaadithyasairam/spine-fracture-prediction-from-xrays. (Accessed 15 November 2022).

[52] N.M. Zaitoun, M.J. Aqel, Survey on image segmentation techniques, Proc. Comput. Sci. 65 (2015) 797–806, https://doi.org/10.1016/j.procs.2015.09.027.

[53] C. Shorten, T.M. Khoshgoftaar, A survey on image data augmentation for deep learning, J Big Data 6 (1) (Dec. 2019) 60, https://doi.org/10.1186/s40537-019-0197-0.
[54] S.G. Paul, et al., Combating Covid-19 using machine learning and deep learning: applications, challenges, and future perspectives, Array 17 (Mar. 2023), 100271, https://doi.org/10.1016/j.array.2022.100271.
[55] E. Mbunge, S. Simelane, S.G. Fashoto, B. Akinnuwesi, A.S. Metfula, Application of deep learning and machine learning models to detect COVID-19 face masks - a review, Sustain. Oper. Comput. 2 (2021) 235–245, https://doi.org/10.1016/j.susoc.2021.08.001.
[56] S.G. Paul, et al., A real-time application-based convolutional neural network approach for tomato leaf disease classification, Array 19 (Sep. 2023), 100313, https://doi.org/10.1016/j.array.2023.100313.
[57] "Confusion Matrix," Wikipedia, Aug. 31, 2022 [Online]. Available: https://en.wikipedia.org/w/index.php?title=Confusion_matrix&oldid=1107701525. (Accessed 26 December 2022).
[58] Showmick, Cervical-Spine-Fracture (Dec. 29, 2022) [Online]. Available: https://github.com/showmick5/Cervical-Spine-Fracture. (Accessed 29 December 2022).